

Optical Outcoupling Efficiency in Polymer Light-Emitting Diodes

Yungui Li,* Bas Van der Zee, Gert-Jan A. H. Wetzelaer, and Paul W. M. Blom*

The electrical properties of polymer-based light-emitting diodes (PLEDs) have been extensively studied, resulting in quantitative device models. However, for a complete description of the optoelectronic properties of a PLED, the obtained recombination profiles need to be integrated with an optical model describing the local outcoupling efficiency of the generated light. In this work, combined electrical and optical model calculations are presented, demonstrating that the light-outcoupling efficiency in PLEDs is governed by the presence of electron traps and the anisotropy factor of optical dipoles. Electron trapping confines the recombination in a region close to cathode, resulting in strong optical trapping in surface plasmon polariton modes. Trap-filling leads to a voltage-dependent recombination profile and optical outcoupling efficiency. For a typical electron trap density of $\approx 10^{23} \text{ m}^{-3}$, the calculated outcoupling efficiency raises from 5.5% at 2 V to 10.4% at 5 V in case of isotropic emitters. For conjugated polymers such as super yellow poly(*p*-phenylene vinylene) with the chains preferentially aligned in the plane of the film, the outcoupling efficiency can reach $\approx 18\%$ at 5 V. Elimination of electron trapping would allow for a further enhancement up to 24%.

1. Introduction

Polymer-based light-emitting diodes (PLEDs) are considered as attractive candidates for large-area flexible displays due to their cost-effective solution processability. In the last three decades, attention has been paid to electrical processes that govern PLEDs performance, such as charge injection, transport, and recombination.^[1] For poly(*p*-phenylene vinylene)-based polymers it was demonstrated that the electron and hole transport are strongly unbalanced due to electron trapping.^[2] By investigating a whole range of polymers it was

found that the trapping was governed by a universal electron trap with an energy of $\approx 3.6 \text{ eV}$ below the vacuum level and a density in the 10^{23} m^{-3} regime.^[3,4] The trapped electrons subsequently recombine with free holes via a non-radiative process that competes with the emissive bimolecular Langevin recombination. Furthermore, the electron trapping confines the emissive Langevin recombination in a region close to the cathode, where quenching of excitons occurs.^[5] With increasing bias, voltage traps are being filled and the recombination zone will move away from the cathode. Meanwhile, the bimolecular Langevin recombination gradually dominates over the trap-assisted recombination with increasing bias. Combination of both effects leads to an increase of the PLED efficiency under increased voltage, as could be quantitatively described by a drift-diffusion-based model.^[1] It should be noted that hole traps can play a similar role. It has recently been found that

an energy window exists inside which organic semiconductors show trap-free charge transport. Typically, hole trapping occurs in materials with an ionization energy higher than 6 eV .^[3] However, since the ionization energy of most light-emitting polymers was designed around $\approx 5 \text{ eV}$ to match the work function of anodes like indium–tin–oxide and poly(3,4-ethylenedioxythiophene) polystyrene sulfonate (PEDOT:PSS) to obtain efficient hole injection, PLED efficiency is mainly hindered by electron trapping. In contrast to the electrical properties the magnitude of the optical outcoupling efficiency of PLEDs and the corresponding role of electron traps has received far less attention.

It is well known that not all light generated in a PLED can propagate out of the device due to the mismatch of refractive index between the polymer, glass substrate, and air. As a result of total internal reflections, a large proportion of the generated photons cannot escape the PLED to air. The waveguiding of the generated light can be divided into three modes, namely the air mode (light that escapes from the substrate into air and is collected), the substrate mode (light that stays in the substrate), and the waveguide mode (light trapped in the ITO/organic layer).^[6] Furthermore, because of the coupling between photons and electrons in metallic electrodes, light trapping as surface plasmon polariton (SPP) modes widely exists in organic LEDs (OLEDs).^[7] As a rule of thumb, following the classical ray

Dr. Y. Li, B. Van der Zee, Dr. G.-J. A. H. Wetzelaer, Prof. P. W. M. Blom
 Max Planck Institute for Polymer Research
 Ackermannweg 10, 55128 Mainz, Germany
 E-mail: liy@mpip-mainz.mpg.de; blom@mpip-mainz.mpg.de

 The ORCID identification number(s) for the author(s) of this article can be found under <https://doi.org/10.1002/aelm.202100155>.

© 2021 The Authors. Advanced Electronic Materials published by Wiley-VCH GmbH. This is an open access article under the terms of the Creative Commons Attribution-NonCommercial-NoDerivs License, which permits use and distribution in any medium, provided the original work is properly cited, the use is non-commercial and no modifications or adaptations are made.

DOI: 10.1002/aelm.202100155

optics, the fraction of light for isotropic emitters in OLEDs dissipating to air can be approximated by^[8]

$$\eta_A \approx \frac{1}{2n_{os}^2} \quad (1)$$

where n_{os} is the refractive index of the organic semiconductor. For a typical value of $n_{os} = 1.7$, $\approx 20\%$ of the generated light is then expected to be collected.

So far, most of the work on optical outcoupling efficiency has been focused on OLEDs based on a multilayer stack of evaporated small molecules. An advantage of multilayer OLEDs is that the thin recombination zone can be placed in a position optimal for the outcoupling efficiency by tuning the thickness of the transport layers.^[9,10] With this strategy, outcoupling efficiencies to air modes in the range of 25–30% can be obtained, representing the ratio of photons escaping the OLED structure to the number of totally generated photons. In such a multilayer device configuration, the position of the recombination zone is known, with the profile typically being approximated by a delta-function.^[11] A combination with electrical modeling is usually not made. We have recently demonstrated that the optical outcoupling efficiency for single-layer evaporated OLEDs,^[11] based on the thermally activated delayed fluorescence emitter 9,10-bis(4-(9H-carbazol-9-yl)-2,6-dimethylphenyl)-9,10-diboranthracene (CzDBA) with a broad recombination zone, can be calculated by integrating the outcoupling efficiency at different positions weighted by the sum-normalized recombination profile.^[12] In this case, the final optical outcoupling to air modes is dependent both on the position-dependent outcoupling at different locations and on the recombination profile as obtained from electrical modeling. Due to the balanced and trap-free electron and hole transport in CzDBA, resulting in a recombination profile that is mainly located in the bulk of the semiconductor, an outcoupling efficiency to the air mode as high as $\approx 26\%$ was obtained for this single-layer OLED.^[12] However, for single-layer polymer LEDs with unbalanced transport the recombination zone is typically confined in a region close to the cathode due to electron trapping. The effect of this confinement on the outcoupling efficiency of PLEDs has not been evaluated until now.

In an earlier study it was demonstrated by numerical optical modeling that for single-layer polymer-based LEDs the outcoupling efficiency can be larger than the limit given by Equation (1).^[6,13] This enhanced outcoupling would require the presence of emitters with emissive dipoles with horizontal preference, positioned at the optimal location in the emission zone. However, a connection between this numerical optical efficiency and recombination profiles of PLEDs from an electrical model has only been made in a semi-empirical way until now. The quenching of excitons by the metallic electrode was investigated by time-resolved photoluminescence on PPV derivatives adjacent to a metallic electrode. The experiments showed that next to the direct quenching of excitons by non-radiative energy transfer to the electrode, diffusion of excitons also occurs into the region near the electrode where excitons are depleted.^[14] As such, the width of the quenching region is determined by the sum of a characteristic energy-transfer range of ≈ 75 nm and the exciton diffusion length, L_D , of 6 nm. Based on these length scales, a distant dependence exciton quenching function was

integrated in the PLED device model.^[14,15] In this way, losses due to SPP modes were empirically taken into account. However, for a complete description of the optoelectronic properties of a PLED, a full numerical optical model considering wavelength dependent refractive indices and emissive dipole orientations needs to be integrated with the electrical device model, including trapping and trap-assisted recombination.

To tackle this problem, we use the well-known conjugated polymer super yellow poly(*p*-phenylene vinylene) (SYPPV) as a model system, because all relevant charge transport parameters including the field- and charge carrier-dependent mobility have been experimentally determined using single carrier devices.^[16] In the framework of the Extended Gaussian Disorder Model, it is possible to precisely simulate the recombination profiles in the SYPPV PLEDs at different voltages. Based on the SYPPV model system, we show that the electron trap density plays an essential role on the optical outcoupling efficiency for PLEDs. This is achieved by numerical simulation of the recombination profile with different trap densities, combined with a position-dependent outcoupling efficiency as a function of the anisotropy factor for the emissive dipoles. The total optical outcoupling is then obtained by integrating over the position-dependent outcoupling efficiency, weighted by the sum-normalized recombination profile. Our model calculations show that in the experimentally relevant range around 10^{23} m^{-3} electron trap concentration the efficiency, η_A , is very sensitive to the absolute trap density. In case of isotropic emitters, the η_A for PLEDs would amount only to 10% due to the confinement of the emission zone at the cathode. However, due to the highly horizontal orientated optical dipoles, the integrated outcoupling efficiency to air modes in SYPPV PLEDs reach $\approx 18\%$, which is coincidentally close to the estimate of $\approx 20\%$ provided by Equation (1). We note that since the electron transport in conjugated polymers is governed by a universal electron trap, located at an energy ≈ 3.6 eV below vacuum with a density in the 10^{17} cm^{-3} regime, and polymers in general have horizontally oriented dipoles, the obtained results for SYPPV are representative for PLEDs in general. Our results further demonstrate that reducing the electron trap density not only enhances the electrical efficiency of PLEDs by reduced trap-assisted combination, but simultaneously enhances the optical outcoupling to a maximum of $\approx 24\%$ in case of mainly horizontally oriented dipoles, as measured for SYPPV.

2. Results and Discussion

2.1. Position-Dependent Optical Outcoupling

For optical dipoles in a thick emissive layer, the power dissipation for each dipole within the device cavity is dependent on the distance to the cathode. As shown in **Figure 1**, the energy coupled to SPP modes decreases gradually when the distance between dipoles and the metallic cathode increases. The SPP coupling between photons and electron gases in the metal serves as one of the major energy loss channels for OLEDs, resulting from the fact that the wave vector of SPP modes is larger than that in free space.^[17] A qualitative comparison of outcoupling to air modes can be done based on the difference in power dissipation from

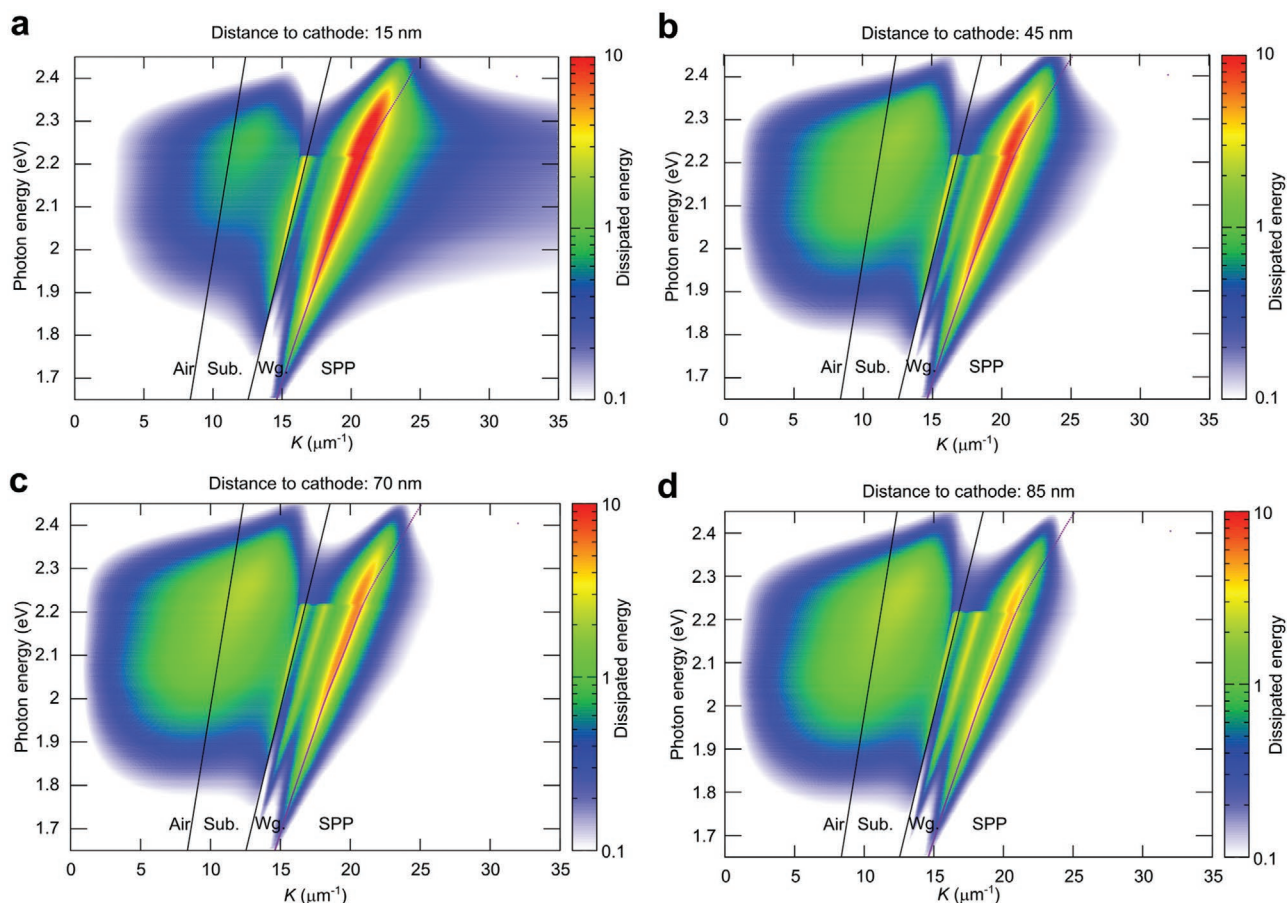


Figure 1. Power dissipation for emissive dipoles at different positions. The simulation is done based on 100 nm PPV polymer, while the emissive interface is treated as a delta function plane. The anisotropy factor is set to 0.333 corresponding to isotropically distributed optical emissive dipoles. The emissive interface has different distances to the metallic cathode: a) 15 nm, b) 45 nm, c) 75 nm, and d) 85 nm. Dissipated modes including air, substrate, waveguide, and SPP modes are indicated according to the parallel wave vector.

emissive dipoles varying distance to the cathode, as shown in Figure 1. However, to reach the maximum photon outcoupling to air, the emissive dipole should be located at an optical position where the sum of SPP modes and the losses as substrate modes and waveguide modes are minimized. We note that the position with the lowest coupling to SPP modes may not be the position with the maximum outcoupling to air modes.

The numerical position-dependent outcoupling efficiency to air modes $\eta_A(x)$ and the sum of air modes and substrate modes $\eta_{SA}(x)$ is shown in Figure 2. Here, optical dipoles are assumed to be isotropically oriented in PLEDs with 100 nm SYPPV as active layer. The maximum η_A of 20.6% can be obtained when emitting dipoles are located at the position with a distance of 70 nm away from the metallic cathode. The maximum η_{SA} of 41.0% can be obtained for dipoles with a distance of 75 nm to the cathode. It is noted that for dipoles at a position only 5 nm away from the cathode, the efficiency, η_A , is only 1.6%. According to our previous results, the final optical outcoupling efficiency for OLEDs with a broad recombination zone can be computed as:^[12]

$$\eta_{\text{out}} = \int_x \eta_{\text{out}}(x) R(x) dx \quad (2)$$

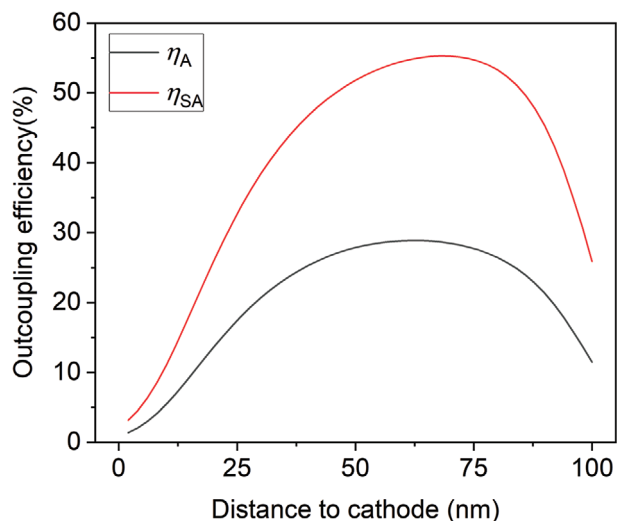


Figure 2. The position-dependent optical outcoupling efficiency with isotropic ($a = 0.333$) dipole moments.

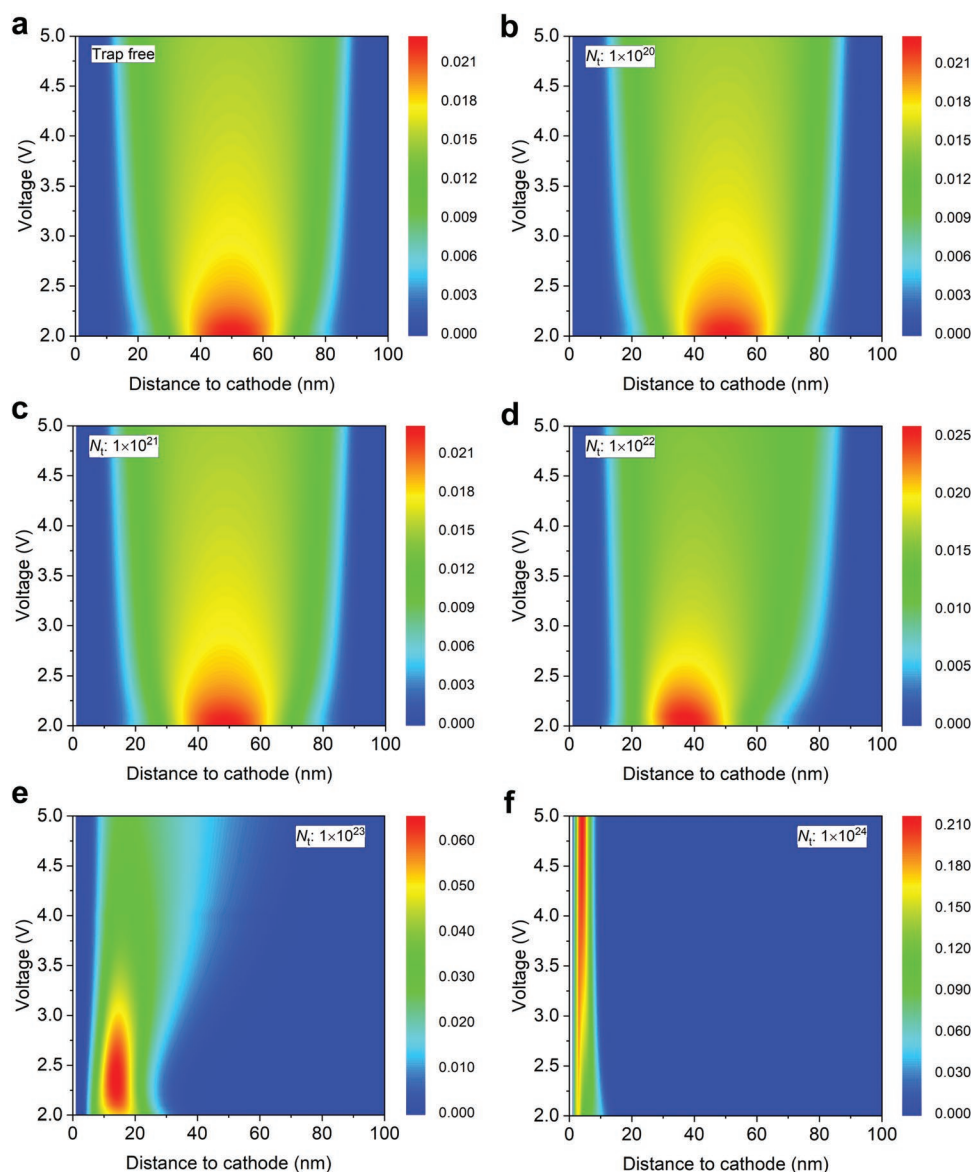


Figure 3. The voltage-dependent recombination profile normalized to the sum for OLEDs with 100 nm polymer with different electron trap densities. The recombination profile is calculated in steps of 1 nm. a) Trap free; b) $1 \times 10^{20} \text{ m}^{-3}$; c) $1 \times 10^{21} \text{ m}^{-3}$; d) $1 \times 10^{22} \text{ m}^{-3}$; e) $1 \times 10^{23} \text{ m}^{-3}$; f) $1 \times 10^{24} \text{ m}^{-3}$.

where $\eta_{\text{out}}(x)$ is the outcoupling efficiency at position x in the recombination zone, while $R(x)$ is the sum-normalized recombination profile. In the following section, we turn to discuss the recombination profile in PLEDs, with SYPPV as a model system.

2.2. Recombination Profile Dependent on Trap Densities

The recombination profile for single-layer PLEDs can be simulated with a drift-diffusion device model developed previously.^[1] The electron trap states are energetically distributed in a Gaussian shape. It has been reported that the electron trap density, N_t , in SYPPV PLEDs typically amounts to 10^{23} m^{-3} . The width of the Gaussian trap distribution amounts to 0.1 eV, and the trap depth equals 0.7 eV.^[16] As a first step, we investigate

the effect of the electron trap density on the recombination profiles and resulting optical outcoupling of the PLED, keeping the remaining device parameters as experimentally determined for SYPPV. As shown in **Figure 3**, the recombination profile is a function of the driving voltage and the trap density N_t . In the absence of traps in the PLED, the recombination profile is symmetrically distributed within the emissive layer. Since the intrinsic charge transport for holes and electrons is balanced,^[1] there is no voltage dependence for the recombination profile in the trap-free case, as shown in Figure 3a. A similar recombination profile is obtained when the trap density is maintained at a low level up to $1 \times 10^{21} \text{ m}^{-3}$, as presented in Figure 3b,c. The trap density in this range is so low that all traps are almost immediately filled before the turn-on voltage, such that it essentially behaves like a trap-free PLED. A more pronounced voltage-dependent recombination profile is observed when

the trap density is further increased to the order of 10^{22} m^{-3} , as shown in Figure 3d and Figure S1, Supporting Information. At low driving voltages, the injected electrons are mainly being trapped, leading to a recombination zone close to the cathode. With increasing voltage, the recombination zone is shifting toward the middle of the device due to trap-filling. However, for trap densities of 10^{23} m^{-3} and beyond, as shown in Figure 3e,f, the voltage dependence of the recombination profile is reduced. For PLEDs with such a higher density of electron traps, the recombination zone stays mainly in the vicinity of the cathode, even at higher driving voltages. For example, for devices with a high electron trap density of $1 \times 10^{24} \text{ m}^{-3}$, the recombination peak is merely 4 nm away from the metallic cathode at 5 V. Combined with Figure 1, it is evident that a significant energy loss occurs via the SPP modes when the recombination zone is so close to the metallic cathode, leading to a very low outcoupling efficiency at high electron trap densities.

2.3. Integrated Optical Outcoupling Weighted by the Recombination Profile

The relation between the trap density and optical outcoupling can be obtained by using Equation (2), where the position-dependent outcoupling efficiency (Figure 2) and the sum-normalized recombination profile, as shown in Figure 3, are combined. The voltage dependence of the outcoupling efficiency to air modes, η_A , using simulated recombination profiles for different trap densities is shown in Figure 4. The corresponding outcoupling efficiency for the sum of air modes and substrate modes, η_{SA} , is shown in Figure S2, Supporting Information. Qualitatively, the higher the electron trap density, the lower the optical outcoupling efficiency. For trap-free devices, the maximum η_A reaches 16.3% with isotropically distributed dipoles, using the optical constants of SYPPV. Similar η_A can also be obtained when the trap density is lower than 10^{21} m^{-3} .

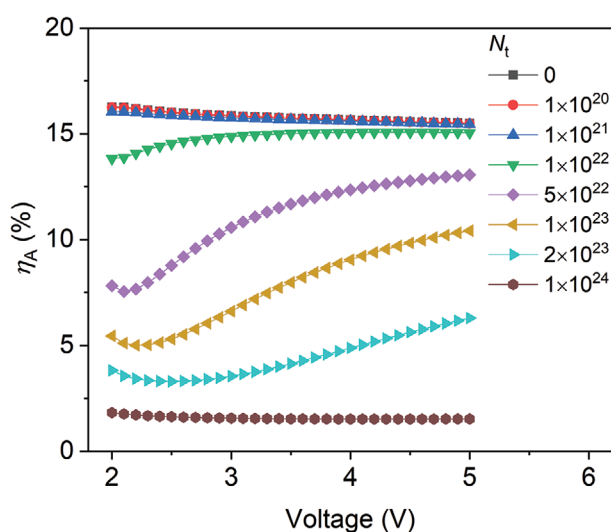


Figure 4. Voltage-dependent η_A for OLEDs with different electron trap densities. The recombination profile is considered. The anisotropy factor is assumed to be 0.333. The trap density has a unit of m^{-3} .

Negligible voltage dependence is observed for such low trap density. For traps with a density in the range from 1×10^{22} to $1 \times 10^{23} \text{ m}^{-3}$, the optical coupling efficiency is very sensitive to the absolute trap density and the applied voltage. The outcoupling efficiency decreases dramatically when the trap density is slightly increased. For isotropic emitters with an electron trap density, N_t , of $1 \times 10^{22} \text{ m}^{-3}$, a maximum η_A of 15.1% is reached at $\approx 4 \text{ V}$, while η_A is only 13.8% at 2 V. For a trap density of $5 \times 10^{22} \text{ m}^{-3}$, the efficiency η_A is gradually increasing from 7.8% at 2 V to 13.1% at 5 V. However, for an increased N_t of $1 \times 10^{23} \text{ m}^{-3}$, the outcoupling efficiency changes from 5.5% at 2 V to 10.4% at 5 V for isotropic optical dipoles. Similar voltage dependence is also found for η_{SA} , as shown in Figure S2, Supporting Information. When the trap density is further increased to $2 \times 10^{23} \text{ m}^{-3}$, the absolute efficiency of η_A further decreases to merely 3.8% at 2 V and 6.3% at 5 V. Finally, the outcoupling efficiency and its voltage dependence is significantly reduced when the trap density reaches $1 \times 10^{24} \text{ m}^{-3}$, resulting from the fact that the recombination zone is almost pinned to the cathode within the investigated driving voltages, as shown in Figure 3f.

According to previous studies, electron trapping in PPV-based devices could be due to water-oxygen clusters.^[3,4,18] Based on our results here, a subtle change of the trap density in this range can, however, result in a significant impact on the recombination profile. The shift of recombination profile can further give rise to a pronounced variation of the optical outcoupling efficiency. It should be noted that such a change in electron trap densities from 0 to $2 \times 10^{23} \text{ m}^{-3}$ would merely give a minor difference to the current density–voltage behavior at room temperature (Figure S3, Supporting Information). This is because the transport is dominated by the trap-free hole transport.

2.4. Horizontal Orientation of PPV Polymers

In previous sections, the optical transition dipole moment is treated isotropic. Such an assumption is valid for many spin-coated organic emitters and thermally deposited films.^[19] In contrast, it has been demonstrated that PPV-based polymers exhibit uniaxial anisotropy because of the preferential horizontal alignment of the polymer chains in the plane of spin-coated films.^[6,20–23] However, the magnitude of the anisotropy factor differs for the various PPV-based polymers.^[19] Considering the universal electron traps in these PPV-based polymers,^[3,4] calculation of the outcoupling efficiency for a range of anisotropy factors would be meaningful for a general investigation for PLEDs, since the anisotropy factor can significantly impact the position-dependent optical outcoupling.^[19,24,25] Therefore, as a first step, we assume that emitters can either be horizontally, isotropically, or vertically oriented. The anisotropy factor of a number of polymeric emitters is then experimentally determined.

As shown in Figure 5a, the position-dependent $\eta_A(x)$ is strongly sensitive to the anisotropy factor. In general, the maximum η_A can be obtained in the middle of the device, when the emissive dipoles are located at the position with a distance of $\approx 60\text{--}70 \text{ nm}$ to the cathode. However, for emitting diodes in the optimal position, the maximum η_A can vary from

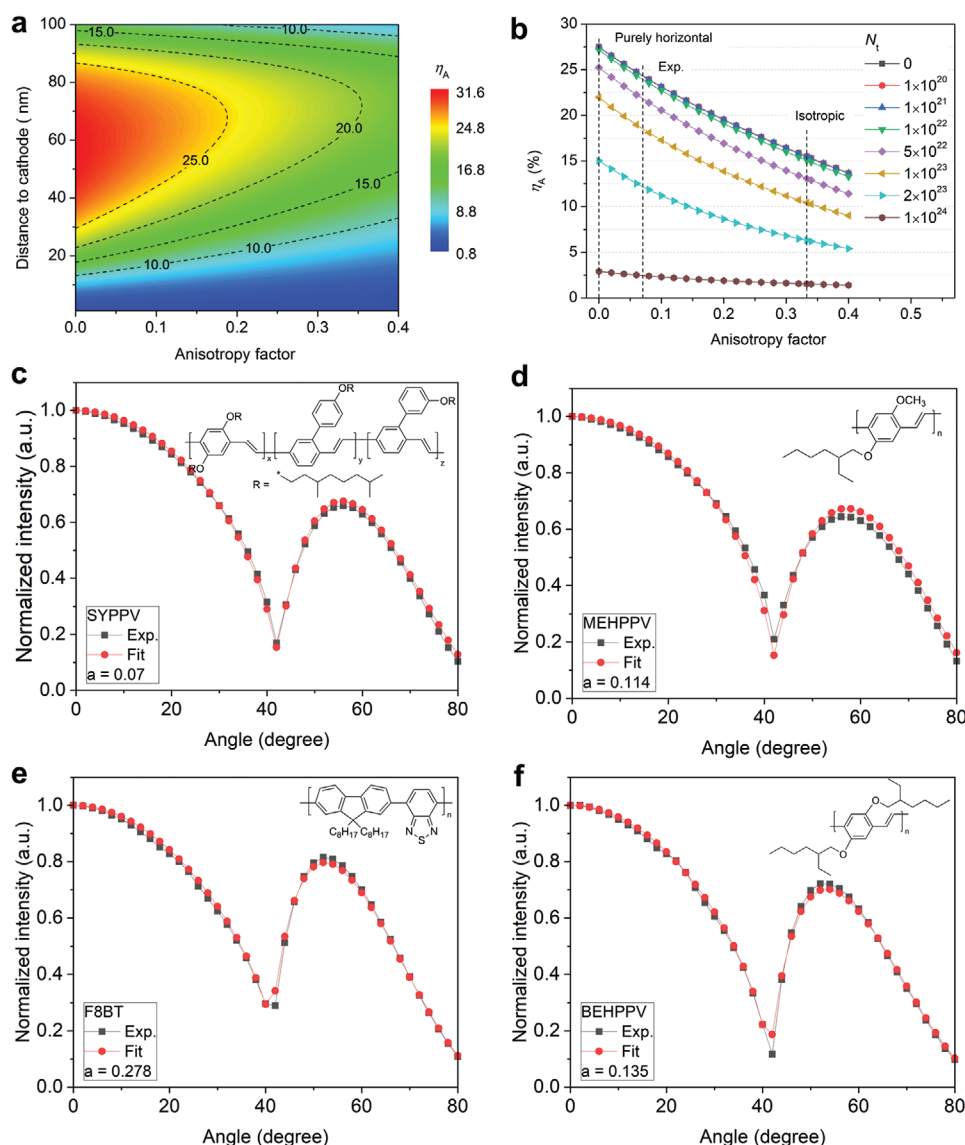


Figure 5. Anisotropy factor dependent optical outcoupling η_A . a) Position-dependent η_A . b) The recombination profile weighted η_A for devices with different electron trap densities (m^{-3}) as a function of anisotropy factor. The simulation here is based on devices with 100 nm SYPPV at 5 V, with the experimental anisotropy factor indicated by a dashed line. c) Anisotropy factor for SYPPV determined from the angular-dependent photoluminescence. d) Anisotropy factor for MEHPPV. e) Anisotropy factor for F8BT. f) Anisotropy factor for BEHPPV. Chemical structures for these polymers are displayed in the insets.

18.7% with an anisotropy factor of 0.4, to 31.6% for purely horizontal dipoles (anisotropy factor of zero). A similar variation is also observed for η_{SA} , as presented in Figure S4, Supporting Information. According to previous studies, emissive dipoles in SYPPV are partially horizontally oriented.^[19,24,25] Experimentally, the anisotropy factor of SYPPV is determined to be as low as 0.07 by polarized angular photoluminescence (Figure 5c). Such a low proportion of vertical dipoles results in lower photon trapping and higher outcoupling efficiency, as compared to isotropically distributed optical dipoles (Figures S5 and S6, Supporting Information). When calculating the optical outcoupling efficiency considering the broad recombination profile, as shown in Figure 5b, the final η_A amounts to $\approx 24\%$ for a PLED with low trap densities ($< 1 \times 10^{22} \text{ m}^{-3}$) and

is in between $\approx 12\%$ and $\approx 18\%$ for PLEDs with a trap density in the range $1\text{--}2 \times 10^{23} \text{ m}^{-3}$, as experimentally observed for SYPPV. The efficiency decreases to $\approx 2\%$ when the trap density increases to $1 \times 10^{24} \text{ m}^{-3}$. Therefore, it is possible for PLEDs to achieve an η_A exceeding $\approx 20\%$, when the trap density is limited to a sufficiently low level.

Previously, the electrical properties including the charge injection, transport, and trap distributions for other polymers, such as poly(9,9-dioctylfluorene-alt-benzothiadiazole) (F8BT), poly[2-methoxy-5-(2-ethylhexyloxy)-phenylene vinylene] (MEHPPV), and poly[2-butoxy-5-(2-ethylhexyloxy)-phenylene vinylene] (BEHPPV), have also been widely investigated.^[3,4] However, the anisotropy factor of their emitting dipoles has not been determined. Here, the anisotropy factor measurements

indicate that the emitters in all these polymers are horizontally preferred in the neat film. As shown in Figure 5d–f, the anisotropy factors amount to 0.114 for MEHPPV, 0.278 for F8BT, and 0.135 for BEHPPV. The anisotropy factor for PPV polymers is much lower compared to reported small molecule-based organic emitters.^[19] Our calculations show that in case of purely horizontal orientation of dipoles and absence of trapping, a maximum optical outcoupling efficiency of $\approx 27\%$ could be possible in a PLED (Figure 5b).

We can also use the model to investigate the outcoupling efficiency of alternative PLED structures as inverted devices. So far, reports on inverted PLEDs are relatively rare; due to the low electron affinity of most conjugated polymers, a reactive metal like Ca or Ba has to be used as cathode. Coating a polymer on top of such a cathode leads to oxidation and reduced performance. Considering the case that an inverted PLED has equally efficient electron injection as with the normal configuration, the recombination profile of the inverted PLEDs is the mirror image of the one with a normal configuration.^[26] Typically, recombination profiles for SYPPV PLEDs both in normal and inverted device configuration are presented in Figures S7a and S7b, Supporting Information, respectively, for various electron trap densities at a bias voltage of 2.5 V. Considering the position dependent optical outcoupling efficiency for SYPPV PLEDs, the final optical outcoupling efficiency at 2.5 V is shown in Figure S7c, Supporting Information. It shows that for SYPPV with low trap density ($<10^{22} \text{ m}^{-3}$), the optical outcoupling efficiency is similar for devices based on either normal or inverted configuration. For devices with high trap density ($>5 \times 10^{22}$ or 10^{23} m^{-3}), the optical outcoupling efficiency of inverted PLEDs is higher than those of normal device configuration, because the recombination zone is close to ITO in inverted PLEDs while it is close to metallic cathode in normal PLEDs. In order to achieve highly efficient PLEDs electron trapping needs to be eliminated to obtain balanced transport and minimize non-radiative trap-assisted recombination. In that case, our modeling shows that changing from a normal to an inverted PLED structure does not bring further advantage with regard to outcoupling efficiency.

3. Conclusion

In conclusion, we have unified numerical, electrical, and optical modeling to fully describe the performance of PLEDs with traps and a voltage-dependent broad recombination profile. We demonstrated the vital importance of trap density on the optical outcoupling in PLEDs. In general, traps in the emissive layer strongly affect the emissive Langevin recombination rate and the recombination profile, which in turn affects the optical outcoupling. For SYPPV devices with a trap density of $1 \times 10^{23} \text{ m}^{-3}$, the outcoupling to air modes is 18% due to the mainly in-plane oriented dipoles, and can reach $\approx 24\%$ for low trap densities. For high trap densities of $1 \times 10^{24} \text{ m}^{-3}$, though uncommon in pristine conjugated polymers, the outcoupling efficiency can be as low as merely 2%. We show that reducing the electron trap density can simultaneously contribute positively to the optical and electrical efficiency to achieve efficient single-layer PLEDs.

4. Experimental Section

Electrical Modeling: The electrical model analysis for the single-layer OLEDs with a layer of 100 nm SYPPV was based on EGDM described previously, with the consideration of electrical energy gap, trap density, and charge carrier mobility.^[1] The charge density and electrical field dependent mobility were described in a numerical manner.^[27] According to the temperature-dependent voltage–current density characterization, the zero field mobility for electrons, μ_{n0} , and holes, μ_{p0} , was set as $600 \text{ m}^2 \text{ V}^{-1} \text{ s}^{-1}$, the lattice constant for electrons, a_n , and holes, a_p , as 1.6 nm, and width of Gaussian density of states for electrons, σ_n , and holes, σ_p , as 0.14 eV.^[16] The voltage–current density behavior, Langevin recombination profile, the intensity of Langevin, and SRH recombination at each voltage could be then simulated.

Optical Modeling: The power dissipation for emissive dipoles at different position within the device was simulated based on the model described by Furno et al.^[11] For the ITO anode, PEDOT:PSS hole injection layer, and Al cathode, reported experimental optical constants were used. The optical constants for SYPPV were obtained from literature.^[28]

Supporting Information

Supporting Information is available from the Wiley Online Library or from the author.

Acknowledgements

The authors thank Prof. Karl Leo and Dr. Mauro Furno for making available the simulation script for OLEDs with a delta-function emissive plane and the application permission for this work.

Open access funding enabled and organized by Projekt DEAL.

Conflict of Interest

The authors declare no conflict of interest.

Data Availability Statement

Data available on request from the authors.

Keywords

broad recombination profiles, Langevin recombination, optical outcoupling, polymer light-emitting diodes, trap-assisted recombination

Received: February 15, 2021

Revised: March 25, 2021

Published online:

- [1] M. Kuik, G.-J. A. H. Wetzelaer, H. T. Nicolai, N. I. Craciun, D. M. De Leeuw, P. W. M. Blom, *Adv. Mater.* **2014**, 26, 512.
- [2] M. M. Mandoc, B. de Boer, G. Paasch, P. W. M. Blom, *Phys. Rev. B* **2007**, 75, 12.
- [3] N. B. Kotadiya, A. Mondal, P. W. M. Blom, D. Andrienko, G. J. A. H. Wetzelaer, *Nat. Mater.* **2019**, 18, 1182.
- [4] H. T. Nicolai, M. Kuik, G. A. H. Wetzelaer, B. de Boer, C. Campbell, C. Risko, J. L. Brédas, P. W. M. Blom, *Nat. Mater.* **2012**, 11, 882.

- [5] D. E. Markov, C. Tanase, P. W. M. Blom, J. Wildeman, *Phys. Rev. B* **2005**, 72, 045217.
- [6] J. S. Kim, P. K. H. Ho, N. C. Greenham, R. H. Friend, *J. Appl. Phys.* **2000**, 88, 1073.
- [7] W. L. Barnes, A. Dereux, T. W. Ebbesen, *Nature* **2003**, 424, 824.
- [8] B. E. A. Saleh, M. C. Teich, *Fundamentals of Photonics*, John Wiley & Sons, Inc., New York **2019**.
- [9] S. Hofmann, M. Thomschke, P. Freitag, M. Furno, B. Lüssem, K. Leo, *Appl. Phys. Lett.* **2010**, 97, 253308.
- [10] R. Meerheim, M. Furno, S. Hofmann, B. Lüssem, K. Leo, *Appl. Phys. Lett.* **2010**, 97, 253305.
- [11] M. Furno, R. Meerheim, S. Hofmann, B. Lüssem, K. Leo, *Phys. Rev. B* **2012**, 85, 115205.
- [12] Y. Li, N. B. Kotadiya, B. Zee, P. W. M. Blom, G. A. H. Wetzelaer, *Adv. Opt. Mater.* **2021**, <https://doi.org/10.1002/adom.202001812>.
- [13] Y. Li, Q. Li, P. W. M. Blom, G.-J. A. H. Wetzelaer, *Appl. Phys. Express* **2021**, 14, 022004.
- [14] D. E. Markov, P. W. M. Blom, *Phys. Rev. B* **2005**, 72, 5.
- [15] D. E. Markov, P. W. M. Blom, *Appl. Phys. Lett.* **2005**, 87, 233511.
- [16] Q. Niu, G. J. A. H. Wetzelaer, P. W. M. Blom, N. I. Crăciun, *Adv. Electron. Mater.* **2016**, 2, 1600103.
- [17] Y. Li, Z. Tang, C. Hänisch, P.-A. Will, M. Kovačič, J.-L. Hou, R. Scholz, K. Leo, S. Lenk, S. Reineke, *Adv. Opt. Mater.* **2019**, 7, 1801262.
- [18] J. M. Zhuo, L. H. Zhao, R. Q. Png, L. Y. Wong, P. J. Chia, J. C. Tang, S. Sivaramakrishnan, M. Zhou, E. C. W. Ou, S. J. Chua, W. S. Sim, L. L. Chua, P. K. H. Ho, *Adv. Mater.* **2009**, 21, 4747.
- [19] T. D. Schmidt, T. Lampe, M. R. D. Sylvinson, P. I. Djurovich, M. E. Thompson, W. Brütting, *Phys. Rev. Appl.* **2017**, 8, 037001.
- [20] C. M. Ramsdale, N. C. Greenham, *Adv. Mater.* **2002**, 14, 212.
- [21] D. McBranch, I. H. Campbell, D. L. Smith, J. P. Ferraris, *Appl. Phys. Lett.* **1995**, 66, 1175.
- [22] M. Tammer, A. P. Monkman, *Adv. Mater.* **2002**, 14, 210.
- [23] C. W. Y. Law, K. S. Wong, Z. Yang, L. E. Horsburgh, A. P. Monkman, *Appl. Phys. Lett.* **2000**, 76, 1416.
- [24] Y. Li, M. Kovačič, J. Westphalen, S. Oswald, Z. Ma, C. Hänisch, P. Will, L. Jiang, M. Junghaehnel, R. Scholz, S. Lenk, S. Reineke, *Nat. Commun.* **2019**, 10, 2972.
- [25] M. J. Jurow, C. Mayr, T. D. Schmidt, T. Lampe, P. I. Djurovich, W. Brütting, M. E. Thompson, *Nat. Mater.* **2016**, 15, 85.
- [26] S. Höfle, A. Schienle, M. Bruns, U. Lemmer, A. Colmann, *Adv. Mater.* **2014**, 26, 2750.
- [27] W. F. Pasveer, J. Cottaar, C. Tanase, R. Coehoorn, P. A. Bobbert, P. W. M. Blom, M. De Leeuw, M. A. J. Michels, *Phys. Rev. Lett.* **2005**, 94, 206601.
- [28] T. Lanz, E. M. Lindh, L. Edman, *J. Mater. Chem. C* **2017**, 5, 4706.